JOURNAL OF CATALYSIS 111, 152–169 (1988)

Solid Electrolyte Aided Study of the Mechanism of CO Oxidation on Polycrystalline Platinum

I. V. YENTEKAKIS, S. NEOPHYTIDES, AND C. G. VAYENAS[1]

Institute of Chemical Engineering and High Temperature Chemical Processes, Department of Chemical Engineering, University of Patras, Patras 26110, Greece

Received July 14, 1987; revised December 7, 1987

The mechanism of CO oxidation on polycrystalline Pt at atmospheric pressure has been investigated by combining kinetic and simultaneous potentiometric studies in a gradientless reactor containing one or two polycrystalline Pt films supported on stabilized zirconia. The initial oxidation state of the catalyst was found to have an important effect both on the steady-state behavior and on the waveform of rate and emf oscillations. A simple kinetic model where both oxygen adsorption and surface reaction are rate limiting is found to describe semiquantitatively the steady-state kinetic and potentiometric results both on preoxidized and on prereduced surfaces. The oscillatory behavior of the system was studied in detail by simultaneous mass spectroscopic monitoring of the concentrations of O_2 and CO_2. The kinetic and potentiometric results suggest strongly that the oscillations are caused by periodic formation and consumption of surface PtO_2. The formation of PtO_2 is verified by a series of surface $CO-O_2$ titration experiments. The experiments with two polycrystalline films show that oscillation synchronization occurs via the gas phase as the two films exposed to the same gaseous environment exhibit synchronous oscillations in the surface oxygen activity.

INTRODUCTION

The oxidation of carbon monoxide on platinum is one of the most thoroughly studied catalytic reactions. Despite a very large number of experimental and theoretical studies there still exists a number of unresolved questions regarding the exact reaction mechanism and the origin of hysteresis, steady-state multiplicity, and limit cycle phenomena observed during the reaction under both atmospheric and low-pressure conditions. Work prior to 1977 had been reviewed by Sheintuch and Schmitz (*1*) and Slin'ko and Slin'ko (*2*). Engel and Ertl have reviewed work on the surface science aspects of the $CO/O_2/Pt$ system (*3*) while some of the mathematical modeling work prior to 1985 has been reviewed by Sheintuch (*4*). In a recent comprehensive review Razon and Schmitz have critically evaluated experimental and modeling work prior to 1985 (*5*).

Before 1980 there were considered to be four major candidates as the cause for oscillations: (a) strong dependence of the activation energy or heat of adsorption on surface coverage (*1, 6, 7*), (b) surface temperature oscillations (*8*), (c) shift between multiple steady states due to slow adsorption or desorption of an inert species (*9*), and (d) periodic oxidation and reduction of the surface (*7, 10, 11*). Mathematical models attempting to describe the oscillatory phenomena were usually based on one or more of the above assumptions. Agreement with experiment was qualitative at best. After 1980 the work of Sales, Turner, Maple, and coworkers (*12–15*) provided experimental and theoretical evidence that the origin of oscillations is most likely related to (d) and to some extent to (c). Their mathematical simulations gave good agreement with experiment (*15*). Similar conclusions were reached for the ethylene oxidation on Pt where it was shown that the bifurcation between oscillatory and nonoscillatory states occurs near the dissociation pressure of

[1] To whom correspondence should be addressed.

0021-9517/88 $3.00

PtO_2 (*16, 18*) and that the oscillations could be modeled successfully with a model taking into account the existence of PtO_x (*17*).

In 1982 Ertl and co-workers (*19*) showed that the reaction can exhibit sustained oscillations on a Pt(100) surface at low pressures (10^{-4} Torr). They used LEED to show that during oscillations the surface undergoes periodic structural transformations between the (1 × 1) phase and a reconstructed hexagonal structure (*20*). A mathematical model was developed which described well the experimental observations (*21*). Subsequent work by two other groups seems to confirm the idea that the origin of oscillations is different at atmospheric pressure and at low pressures: Yeates *et al.* (*22*) used LEED, AES, and a Kelvin probe to study the reaction on single crystals at low pressures and also at atmospheric pressure. They confirmed the low-pressure findings of Ertl and co-workers (*21*) but found strong evidence that at atmospheric pressure the oscillations are caused by formation and destruction of surface platinum oxide. Similar conclusions were reached by Lindstrom and Tsotsis (*23*) who studied the reaction over both single-crystal Pt(100) and supported catalysts at intermediate (1–10 Torr) pressures.

The first detailed study of the thermodynamics and kinetics of formation of surface platinum oxide was carried out by Berry (*24*). The dissociation pressure of platinum oxide reported by Berry was found to correlate well with the solid electrolyte aided measurements of surface oxygen activity at the bifurcation point between oscillatory and nonoscillatory states during ethylene oxidation on platinum (*16, 18*). Riekert (*35*) has shown qualitatively how surface oxides can give rise to rate oscillations, and mathematical models which take into account the existence of surface platinum oxide have described well the limit cycle phenomena during ethylene (*17*) and CO (*15*) oxidation on Pt. Recent UHV work by Peuckert and Ibach (*25*) and Peuckert and Bonzel (*26*), who used XPS, AES, and EELS on clean Pt surfaces, has positively confirmed the existence of surface PtO_2. Good agreement has been reported (*26*) between their UHV results and the dissociation pressure of Berry and Vayenas and co-workers. In a recent study Hafele and Lintz used solid electrolyte potentiometry (SEP) to show that platinum oxide formation is thermodynamically possible during CO oxidation on platinum (*29, 30*). They used *ex situ* XPS to show that PtO_2 formation takes place and hinders the rate of CO oxidation. Solid electrolyte cells similar to those used in the present study have already been used by other workers to monitor emf oscillations during CO oxidation on Pt (*27, 28*). Originally proposed by Wagner (*31*) the technique of solid electrolyte potentiometry has been used in conjunction with kinetic measurements to study a number of catalytic oxidations on Pt and on Ag (*16, 32, 33*).

In the present paper we present detailed kinetic and *in situ* surface oxygen activity SEP results obtained in a gradientless reactor under atmospheric pressure conditions. Particular attention was paid to defining the initial oxidation state of the catalyst which was found to play an important role in the catalyst behavior. Similarly to the case of ethylene oxidation on Pt (*16–18*) it is found that the high-frequency bifurcation between oscillatory and nonoscillatory states occurs near the dissociation pressure of PtO_2 (*18, 24*) which strongly supports the idea that PtO_2 formation and decomposition is responsible for the oscillations. This is also supported by surface $CO–O_2$ titration results which show two types of oxygen bonded to the surface. Finally the problem of catalyst crystallite communication and synchrony was addressed by a series of experiments where two catalyst films were used in the same reactor. The SEP measurements showed synchronous oscillations on both films which demonstrates that communication takes place by fast mass transfer via the gas phase.

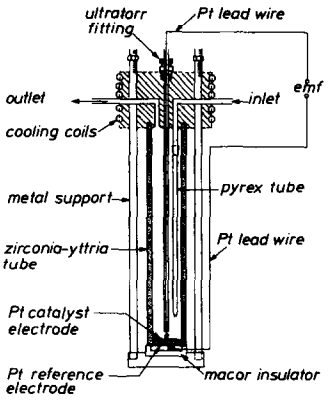

FIG. 1. Schematic diagram of the cell reactor.

EXPERIMENTAL METHODS

Catalyst and Apparatus

The kinetic and potentiometric studies were carried out in the zirconia continuous flow reactor shown in Fig. 1. The reactor has been shown to be well mixed (CSTR) over the range of flow rates used in the present study by obtaining the reactor residence time distribution with a nondispersive IR CO_2 analyzer (*16*). The volume of the reactor was 30 cm^3.

The porous Pt catalyst film was deposited on the flat bottom of a stabilized zirconia tube (8 mole% yttria-stabilized zirconia) by applying a thin coat of Engelhard Hanovia A 1121 platinum paste, followed by drying and calcining in air at 750°C for 2 h and subsequent treatment in a boiling 1 *N* HNO_3 solution for 2 h to remove surface impurities, primarily Bi which is frequently detected in Pt paste electrodes (*29*). The Pt film, approximately 5 μm thick, was examined *ex situ* with XPS using an Al $K\alpha$ source (1486.6 eV). The only detectable impurities were C and O both before and after reaction (*42*). The superficial surface area of the film was 2 cm^2. The true surface area, too low to be measured accurately by BET, was measured by a chemical titration technique using an IR CO_2 analyzer as described in detail below. The same titration technique has been used in studies of ethylene oxidation on Pt (*16*) and Ag (*32*).

In order to address the problem of oscillation synchronization a series of experiments was performed in which two porous Pt catalyst films were deposited on the inside of the flat bottom of the stabilized zirconia tube as shown in Fig. 2a. The superficial surface area of each film was approximately 0.5 cm^2 and each was connected to a different Pt wire so that the electrical potentials of both catalyst–electrodes could be continuously and simultaneously monitored.

A similar porous Pt film was deposited on the outside bottom wall of the stabilized zirconia tube. This Pt film was exposed to air and served as the reference electrode. In some experiments where the exchange current density i_0 was measured by passing current through the cell a second electrode was deposited on the outside bottom wall of the zirconia tube and served as a counter electrode. In this case the reference electrode was very small and was located 5 mm from the counter electrode (Fig. 2b).

The open end of the stabilized zirconia tube was clamped to an appropriately machined stainless-steel reactor cap. The cap had provisions for introduction of reactants and removal of products through Pyrex tubes and also for introduction of one or two Pt wires partly enclosed in Pyrex or α-Al_2O_3 tubes to establish electrical contact

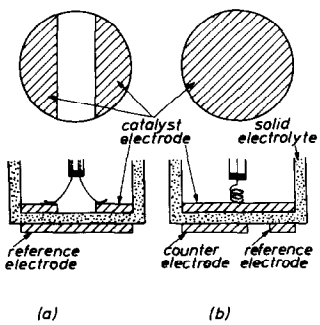

FIG. 2. Electrode configuration for the measurement of the open-circuit emfs with two catalyst–electrodes (a) and for emf measurement and O^{2-} pumping with one catalyst–electrode (b).

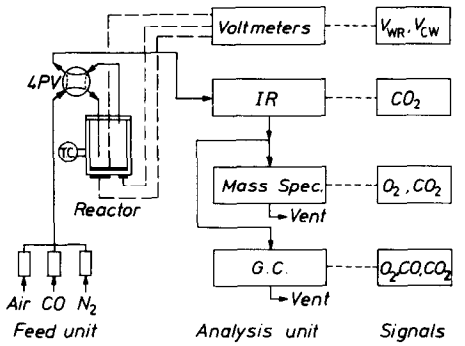

FIG. 3. Schematic diagram of the apparatus.

with the internal Pt film catalyst electrode(s).

The open-circuit emf of the oxygen concentration cell was measured with a solid-state differential volt meter (J. Fluke Model 891 A) which had an input impedance of 10^8 Ω and infinite resistance at null. The catalyst temperature was controlled within 2°C and also measured with a second thermocouple attached to the wall of the stabilized zirconia tube at a distance of 1 mm from the outside electrode.

The reactants were Linde standard CO diluted in N_2 and Linde standard synthetic air. They could be further diluted with ultrapure (99.999%) N_2. It was found necessary to preheat the reactants at 350°C in a spiral Pyrex tube placed before the reactor in order to completely decompose Fe carbonyl formed in the CO cylinder over long periods of time.

As shown in Fig. 3 reactants and products were analyzed by three independent techniques.

(a) On-line gas chromatography for CO, CO_2, O_2, and N_2 using a Perkin–Elmer sigma-2 gas chromatograph with a TC detector. A Porapak Q column was used to separate air and CO_2 and a molecular sieve 5A column was used to separate N_2, O_2, and CO.

(b) On-line mass spectroscopy using a Balzers QMG311 quadrapole mass spectrometer with a QDP101 data processor which made it possible to monitor simultaneously the reactor exit concentrations of CO_2 and O_2. This turned out to be essential for the study of the oscillations.

(c) On-line IR spectroscopy using a Beckman Model 864 nondispersive CO_2 analyzer with a response time of 0.5 s which gave a higher sensitivity to the effluent CO_2 signal than the mass spectrometer due to the unavoidable vacuum system background noise at AMU 44.

Surface Titrations

In order to determine the surface area of the porous Pt catalyst films the following chemical titration scheme was used (*16, 32, 33*). Oxygen was allowed to chemisorb on the catalyst at some temperature T by passing through the reactor synthetic air for a time t_{O_2}. The reactor was subsequently purged with high-purity N_2 for a time t_{N_2} at least eight times longer than the residence time of the CSTR (~6 s). Then the reactor was purged with CO and the total amount of CO_2 formed was determined by the IR CO_2 analyzer. By varying t_{N_2} one can study the kinetics of oxygen desorption from Pt, which are much slower than the CO–oxygen reaction kinetics. By extrapolating to $t_{N_2} = 0$ one can determine the maximum number n_O^0 of oxygen g atoms adsorbed on the catalyst (Fig. 4).

The same procedure can be used by preadsorbing CO for a time t_{CO}, purging with N_2 for a time t_{N_2}, and then purging with O_2 and measuring the total amount of CO_2 formed. By extrapolating again to $t_{N_2} = 0$ one can determine the maximum number n_{CO}^0 of CO moles adsorbed on the catalyst (Fig. 4); n_{CO}^0 was thus estimated to be 3.6×10^{-7} and 2.4×10^{-7} moles, respectively, for reactors 1 and 2.

In the course of the experiments it was found that the time of catalyst exposure to O_2, t_{O_2}, has an increasing effect on n_O^0. This increase is more pronounced at temperatures above roughly 360°C. Furthermore it was found that for large t_{O_2}, i.e., several

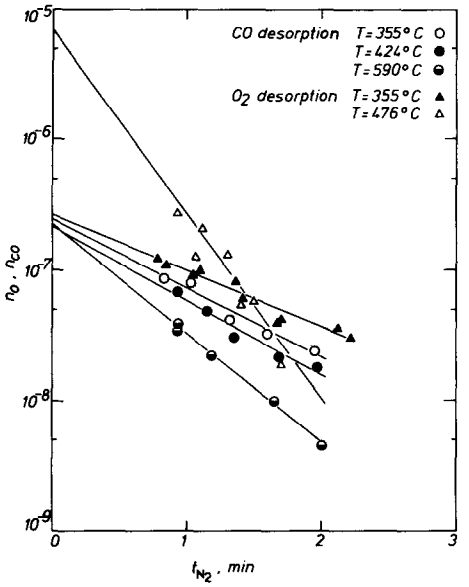

FIG. 4. Typical results of surface titrations during CO and oxygen desorption after catalyst exposures of t_{CO} = 240 s and t_{O_2} = 100 s, respectively; reactor 2.

hours, n_O^0 could exceed n_{CO}^0 by more than a factor of 10 (Fig. 4), which strongly suggests the possibility of multilayer oxidation of the Pt surface. This is corroborated by the appearance of two distinct peaks on the output of the IR CO_2 analyzer upon CO reaction with a preoxidized Pt surface as shown under Results and Discussion. It was therefore concluded that only n_{CO}^0 provides an unambiguous measure of the surface area of the catalyst.

Potentiometric Measurements

The measurement of the open-circuit emf E of solid electrolyte cells in which one electrode is also used as a catalyst can give useful *in situ* information about the activity of oxygen adsorbed on the catalyst–electrode. This simple technique of solid electrolyte potentiometry (SEP) was originally proposed by Wagner (*31*) and has been used in conjunction with kinetic measurements in numerous studies of catalytic oxidations on metals (*16, 17, 27, 28, 30, 32, 33*). Progress regarding the use of solid electrolyte cells to study and to influence catalytic phenomena on metal surfaces has been reviewed recently (*45*).

The open-circuit emf E of the solid electrolyte cell utilized here is

$$E = [1/4F][\mu_{O_2(Pt)catalyst} - \mu_{O_2(Pt)reference}], \quad (1)$$

where F is the Faraday constant and $\mu_{O_2(Pt)}$ is the chemical potential of oxygen adsorbed on the Pt electrodes. This is derived on the assumption that the stabilized zirconia solid electrolyte is a purely anionic (O^{2-}) conductor and that the dominant exchange current reaction involves O^{2-} and adsorbed oxygen. In the CO oxidation system studied here the possibility of other exchange current reactions (e.g., $CO + O^{2-} \rightleftharpoons CO_2 + 2e^-$) that would create mixed potentials cannot be excluded under fuel-rich conditions where most of the catalyst electrode surface is covered with CO (*28, 36*). Consequently under fuel-rich conditions it is possible that the emf E provides only a qualitative measure of the surface oxygen activity (*36, 38*). Equation (1) includes as a limiting case the usual Nernst equation

$$E = (RT/4F) \ln(p'_{O_2}/p_{O_2}), \quad (2)$$

which is valid only when no chemical reaction involving the gas phase takes place at the electrode surface (*16*). In the general case it is the activity of absorbed species rather than the gas phase activities which determines the open-circuit emf (*16, 31–33*). The chemical potential of oxygen at the reference electrode which is in contact with air (p_{O_2} = 0.21 bar) is given by

$$\mu_{O_2(Pt)reference} = \mu^0_{O_2(g)} + RT \ln(0.21), \quad (3)$$

where $\mu^0_{O_2(g)}$ is the standard chemical potential of oxygen at the temperature of interest. Since at temperatures of catalytic interest oxygen is well known to chemisorb dissociatively on Pt, one can define the activity of oxygen atoms on the catalyst a_O by a similar equation,

$$\mu_{O_2(Pt)catalyst} = \mu^0_{O_2(g)} + RT \ln a_O^2. \quad (4)$$

Consequently a_O^2 expresses the partial pressure of gaseous oxygen that would be in thermodynamic equilibrium with oxygen atoms adsorbed on the platinum surface, if such an equilibrium were established.

Combining (1), (3), and (4), a_O ($bar^{1/2}$) is given by

$$a_O = (0.21)^{1/2} \exp(2FE/RT). \qquad (5)$$

If equilibrium is established during reaction between gaseous oxygen in the reactor and surface oxygen, then $a_O^2 = p_{O_2}$. As previously noted Eqs. (1) and (5) may not be exactly valid under fuel-rich conditions where the coverage of adsorbed CO is high and the open-circuit emf E takes values below −300 mV (*28, 36*). Consequently in the fuel-rich region the emf measurement E and the corresponding a_O values obtained by using Eq. (5) provide only a qualitative measure of the oxidation state of the catalyst.

RESULTS AND DISCUSSION

Kinetic Measurements and Rate Oscillations

The steady-state kinetics and oscillatory behavior were studied at temperatures between 200 and 450°C, CO partial pressures up to 0.025 bar, and oxygen partial pressures up to 0.2 bar. The zirconia tube itself, before deposition of the Pt electrode, was totally inactive for CO oxidation even at 450°C.

The inlet stream impinged on the catalyst film through a narrow orifice at the end of the Pyrex feed tube with velocities of order 1–2 m/s to avoid external diffusional limitations. Diffusional limitations inside the porous Pt film were also negligible because of the very small film thickness ($L \approx 5$ μm). Assuming a catalyst porosity of 0.5 and tortuosity of 2, one can estimate the catalyst Thiele modulus $\phi = L(K/De)^{1/2}$ to be less than 0.2 under all conditions studied.

During the kinetic measurements particular emphasis was given to defining the initial oxidation state of the catalyst, since this was found to have a pronounced and reproducible effect on the kinetic behavior. This is something which has been neglected in many kinetic studies in the past and can cause confusion about the kinetics and an apparent irreproducibility in the steady-state and oscillatory catalyst behavior. Kinetic measurements were obtained after leaving the catalyst overnight at the temperature of interest either in air or in CO. We will refer to the two cases as a preoxidized and a prereduced catalyst.

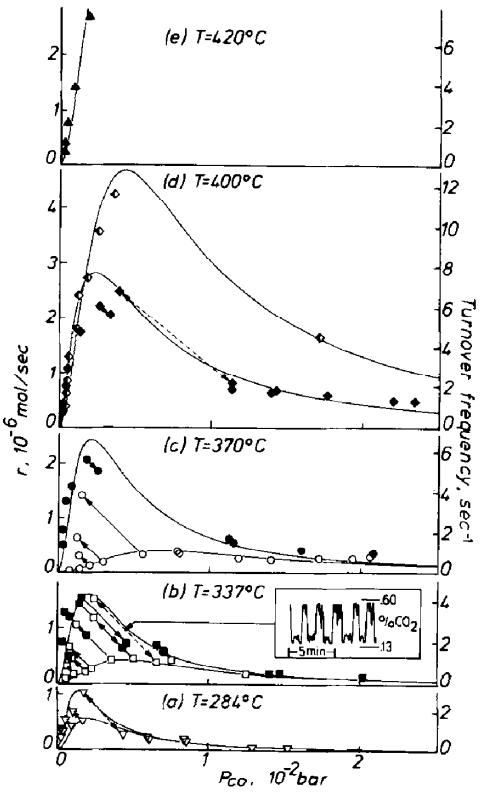

FIG. 5. Effect of p_{CO} on reaction rate at quasi-constant exit p_{O_2}: (a) $p_{O_2} = 5.26 \times 10^{-2}$ bar, total molar flow rate $F = 2.72 \times 10^{-4}$ mole/s; (b) $p_{O_2} = 5.43 \times 10^{-2}$ bar, $F = 2.72 \times 10^{-4}$ mole/s; (c) $p_{O_2} = 5.28 \times 10^{-2}$ bar, $F = 2.72 \times 10^{-4}$ mole/s; (d) (♦) $p_{O_2} = 1.37 \times 10^{-2}$ bar, $F = 2.60 \times 10^{-4}$ mole/s, (◆) $p_{O_2} = 4.62 \times 10^{-2}$ bar, $F = 3.38 \times 10^{-4}$ mole/s; (e) $p_{O_2} = 4.59 \times 10^{-2}$ bar, $F = 3.38 \times 10^{-4}$ mole/s; reactor 1. Solid curves from model.

Figure 5 shows typical kinetic results obtained at constant exit p_{O_2}. The solid curves were obtained from the kinetic model discussed below. The filled and open symbols

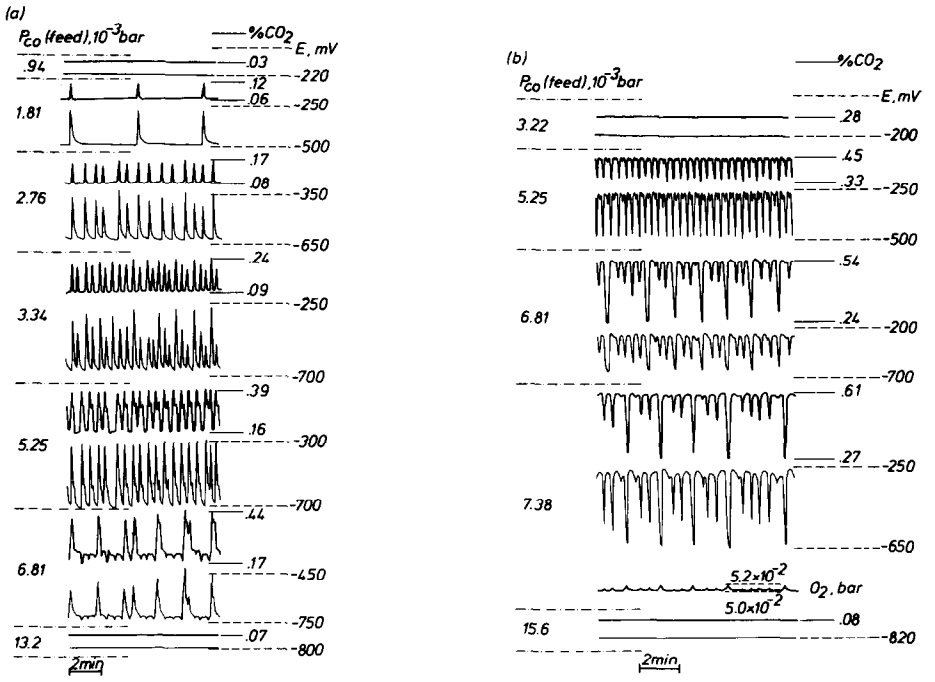

FIG. 6. Effect of inlet p_{CO} at constant inlet $p_{O_2} = 5.43 \times 10^{-2}$ bar on the rate and emf oscillations corresponding to Fig. 5b. (a) Type A oscillations, obtained on a preoxidized surface. (b) Type B oscillations, obtained on a prereduced surface. $T = 337$°C, $F = 2.72 \times 10^{-4}$ mole/s; reactor 1.

stand for data obtained on a prereduced and a preoxidized catalyst, respectively. It should be noted that the distinction between the steady-state kinetic behaviors of a preoxidized and a prereduced surface disappears at temperatures roughly above 400°C (Figs. 5d and 5e). At these high temperatures the catalyst surface has a short memory, as it responds quickly to changes in the composition of the reactant gas mixture. However, at lower temperatures (<400°C) there is a strong memory effect. The oscillatory states shown in Figs. 5a, 5b, and 5c were found to be stable for periods of several days. As shown below, these oscillatory states are of two types, for identical gaseous compositions, depending on the initial oxidation state of the catalyst. The oscillatory states of Fig. 5b are shown in Fig. 6, which also shows the corresponding emf oscillations. It should be noted that in all oscillations increasing rate always corresponds to increasing surface oxygen activity, i.e., increasing emf, which is exactly the opposite of the behavior observed during ethylene oxidation on Pt (*16, 17*). The slope of the oscillation arrows in Fig. 5 is uniquely determined by the residence time in the CSTR. Thus all the arrows fall on constant operation lines of the CSTR.

Figure 6 and the corresponding arrows in Fig. 5b show that oscillations occurring on a preoxidized surface are of the relaxation type with rate spikes "up" (Fig. 6a), contrary to oscillations occurring under almost identical gas phase conditions on a prereduced surface, where rate spikes "down" (Fig. 6b) are observed. We will refer to the former case as type A oscillations and to the latter case as type B oscillations. It is worth noting from Fig. 5 that the baseline of oscillations on a prereduced surface is substantially higher than the baseline of oscillations on a preoxidized surface and that

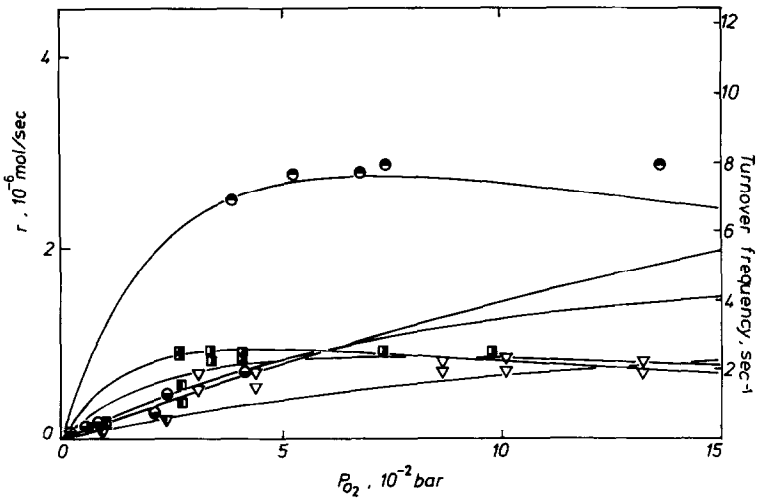

FIG. 7. Effect of p_{O_2} on reaction rate at constant exit p_{CO}: (◒) $T = 370°C$, $p_{CO} = 8.7 \times 10^{-3}$ bar, $F = 3.38 \times 10^{-4}$ mole/s; (◓) $T = 370°C$, $p_{CO} = 1.2 \times 10^{-3}$ bar, $F = 3.38 \times 10^{-4}$ mole/s; (◧) $T = 337°C$, $p_{CO} = 2.8 \times 10^{-3}$ bar, $F = 2.88 \times 10^{-4}$ mole/s; (◨) $T = 337°C$, $p_{CO} = 7.3 \times 10^{-4}$ bar, $F = 2.88 \times 10^{-4}$ mole/s; (▼) $T = 284°C$, $p_{CO} = 3.4 \times 10^{-3}$ bar, $F = 2.88 \times 10^{-4}$ mole/s; (▽) $T = 284°C$, $p_{CO} = 1.7 \times 10^{-3}$ bar, $F = 2.88 \times 10^{-4}$ mole/s; reactor 1. Solid curves from model.

these baselines are usually reached but never traversed by spikes originating from the other baseline. This shows that the rate always oscillates between the limits corresponding to the rates on a preoxidized and prereduced surface. The same limits apply to the aperiodic and probably chaotic states shown in Fig. 6a for high inlet p_{CO} which are similar to those observed and analyzed by other works (*37*). As shown in Fig. 6 increasing p_{CO} at constant p_{O_2} has an increasing effect on the frequency of type A oscillations and a decreasing effect on the frequency of type B oscillation.

The dotted lines in Figs. 5a, 5b, and 5d correspond to oscillations of the type described by Sales and co-workers (*14, 15*). The corresponding waveform is shown in Fig. 5b. It should be noted that these (type "AB") oscillations usually appear when the CSTR operating line can intersect the kinetic curve in more than one point, i.e., in the region of classical steady-state multiplicity in a CSTR.

Figure 7 shows the effect of p_{O_2} at constant p_{CO} on the rate of the reaction. The curves shown on the figure are again obtained from the model discussed below. As shown in Figs. 8a and 8b increasing p_{O_2} increases the frequency of type A oscillations until a maximum is reached after which the frequency decreases. Increasing p_{O_2} always increases the frequency of type B oscillations.

As shown in Fig. 5, oscillations disappear above 400°C over the range of gaseous compositions studied. The upper and lower temperature limits for oscillations were found to increase with increasing p_{CO}/p_{O_2} values (*42*) in agreement with previous studies (*12–15*).

Potentiometric Results

The correct performance of the solid electrolyte cell was verified by introducing into the reactor various air–N_2 mixtures of known oxygen partial pressure and measuring open-circuit emfs in agreement with the Nernst equation

$$E = (RT/4F) \ln(p_{O_2}/0.21) \qquad (6)$$

within ±2 mV. Below 260°C very long times were necessary for the establishment of steady-state emf measurements and no

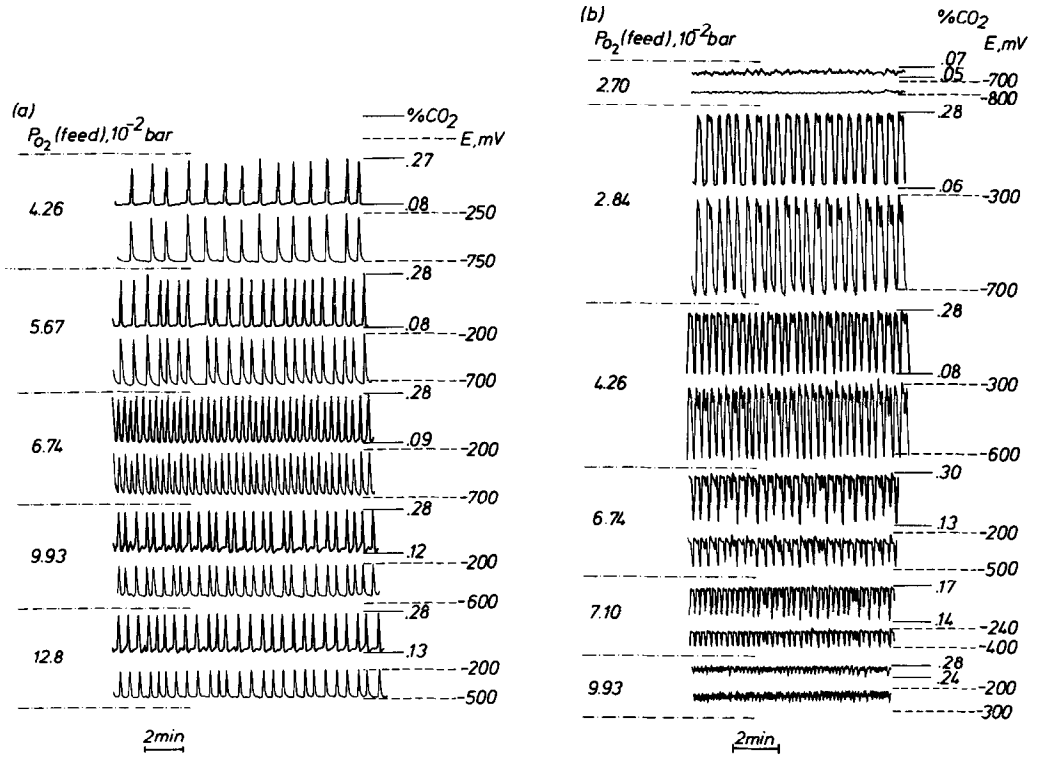

FIG. 8. Effect of inlet p_{O_2} on the rate and emf oscillations at constant inlet $p_{CO} = 3.85 \times 10^{-3}$ bar. (a) Type A oscillations, obtained on a preoxidized surface. (b) Type B oscillations, obtained on a prereduced surface. $T = 337$°C, $F = 2.88 \times 10^{-4}$ mole/s; reactor 1.

data were taken in this region. Catalyst exposure to air–CO mixtures results in open-circuit emfs of −50 to −950 mV, indicating that the surface oxygen activity a_O given by Eq. (5) is quite low and $a^2 < p_{O_2}$. Therefore under reaction conditions adsorbed oxygen is not in thermodynamic equilibrium with gaseous oxygen. It was observed that a_O decreases with increasing p_{CO} and increases with increasing p_{O_2} and that there is a sharp discontinuity in the value of a_O at the point where oscillations occur, indicating that a_O in the fuel-lean region is substantially higher than that in the fuel-rich region. It was found that, as shown by the straight lines in Fig. 9, the steady-state a_O values in both the fuel-lean and the fuel-rich regions can be correlated rather well by

$$a_O = K_l p_{O_2}/p_{CO} \qquad (7a)$$

in the fuel-lean region and by

$$a_O = K_r p_{O_2}/p_{CO} \qquad (7b)$$

in the fuel-rich region. The parameters K_l and K_r increase with temperature and can be approximated by

$$K_l = 6.9 \times 10^3 \exp(-25800/RT) \quad \text{and} \quad K_r = 1.2 \times 10^{-4} \exp(-29000/RT) \qquad (8)$$

with $R = 1.987$ cal/mole · K. Equations (7) and (8) were found to provide a satisfactory fit to the steady-state emf data under both fuel-lean and fuel-rich conditions over a wide range of gaseous compositions, i.e., p_{CO}/p_{O_2} values in the CSTR varying between 10 and 10^{-2}. In the intermediate gaseous composition region, where oscillations take place, catalyst pretreatment affects the emf behavior as already discussed and as shown in Fig. 9. The open symbols in Fig. 9 correspond to a preoxidized catalyst and to the corresponding

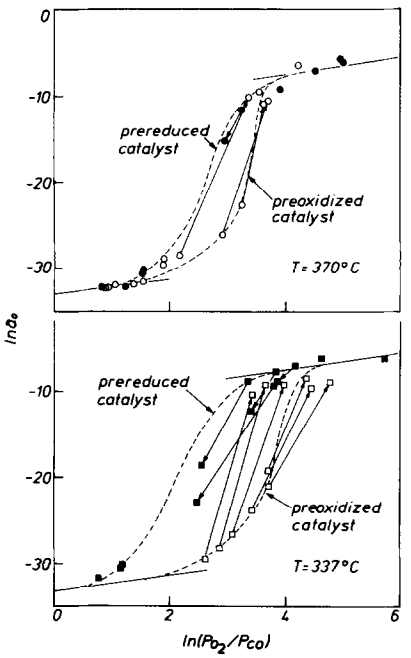

FIG. 9. Effect of gaseous composition and catalyst pretreatment on a_O at steady state and during oscillations. Open and filled symbols indicate preoxidized and prereduced surface, respectively. Arrows pointing up and down indicate types A and B oscillations, respectively.

type A oscillations, while the filled symbols designate a prereduced surface and the corresponding type B oscillations.

Figure 10 shows the dependence of oscillation frequency and amplitude on a_O. It can be seen that the high-frequency bifurcation between oscillatory and nonoscillatory states is near the dissociation pressure of surface PtO_2. Exactly the same behavior has been observed during ethylene oxidation on Pt (*16–18*). This observation which is valid both for type A and type B oscillations (Fig. 10) strongly suggests that surface platinum oxide plays an important role in the oscillatory behavior of ethylene, CO, and possibly other catalytic oxidations on Pt as well. It should be noted that the high-frequency bifurcation between oscillatory and nonoscillatory states near the dissociation pressure of surface PtO_2 occurs well inside the fuel-lean region where the correspondence between the emf E and the surface oxygen activity a_O given by Eq. (5) is unambiguously valid.

Surface Titrations and PtO_2

The dual nature of oxygen on the Pt catalyst is manifested in Figs. 11 and 12 which show two distinct CO_2 peaks upon CO reaction with the catalyst previously exposed to O_2 for varying t_{O_2}. The first peak clearly corresponds to the most reactive form of oxygen, i.e., dissociatively chemisorbed oxygen. The second peak must correspond to surface and subsurface platinum oxide PtO_2. The existence of such an oxide,

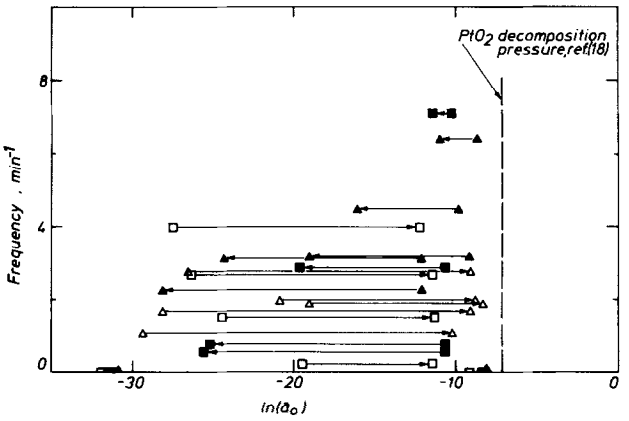

FIG. 10. Effect of a_O on the frequency and amplitude of type A (open symbol) and type B (filled symbols) oscillations. Points correspond to those shown in Figs. 5b, 6 (□), and 8 (△). Conditions as in these figures.

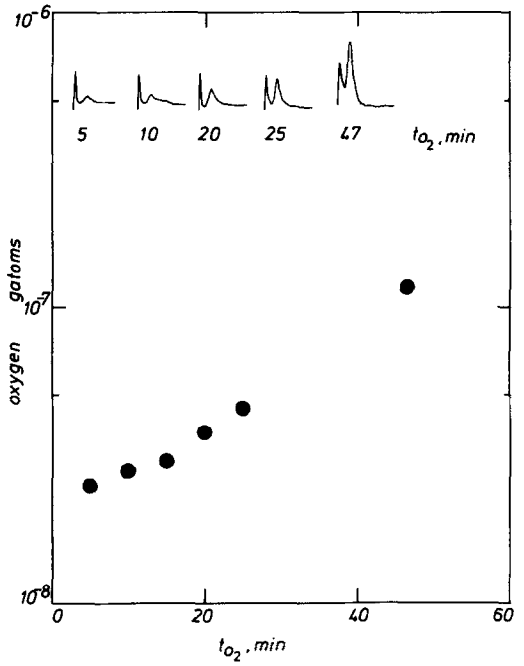

FIG. 11. Effect of catalyst exposure to oxygen t_{O_2} on the total amount and form of surface oxygen found on the catalyst after flushing with N_2 (t_{N_2}) for 105 s. The two forms of oxygen are shown as obtained in the signal of the IR CO_2 analyzer upon flushing with CO. T = 388°C; reactor 3.

which had been invoked to explain rate oscillations during ethylene (*16–18*) and CO (*12–15, 30*) oxidation on Pt, has been verified in a number of studies (*24–26*) using a variety of techniques which include high-precision resistance measurements (*24*), gravimetric techniques (*14*), TPD (*34*), and more recently XPS and Auger studies on clean Pt surfaces (*25, 26*). Its dissociation pressure has been reasonably well established (*16, 18, 24, 25*) and the kinetics of its formation and decomposition have been studied by Berry (*24*) and more recently by Sales *et al.* (*14*) using gravimetric techniques. It is likely that these kinetics can be influenced by Ca and Si impurities (*5, 22*). A difference between the results of (*14*) and the ones presented here is in the amount of PtO_2 that can form on a Pt surface. While in (*14*) no experimental evidence is presented for multilayer oxidation, it is clear from Figs. 4, 11, and 12 that the amount of PtO_2 formed can be considerably higher than the amount corresponding to monolayer coverage. Similar conclusions have been reached by Berry (*24*). As shown in Figs. 11 and 12 chemisorbed oxygen adsorbs and desorbs faster than PtO_2. It is likely that most of the chemisorbed oxygen found at long titration times t_{N_2} (Fig. 12) comes from PtO_2 decomposition which must, as a first step, create dissociatively chemisorbed oxygen. This explains well the observed break in the chemisorbed oxygen desorption curve and the fact that after the break this curve parallels the PtO_2 desorption curve (Fig. 12).

From the slope of the PtO_2 desorption curve (Fig. 12) a kinetic constant of 6×10^{-3} s^{-1} is computed at 388°C. It is interesting to compare this value with the values reported by Turner and Maple (*46*) and Yeates *et al.* (*22*) for PtO_2 reduction by CO. The interpolated values from these refer-

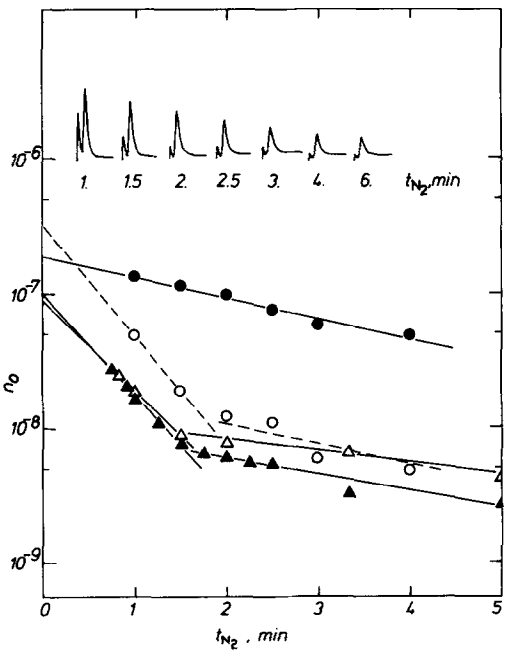

FIG. 12. Effect of desorption time t_{N_2} on the total amount of oxygen n_O found on the surface (triangles) (▲, t_{O_2} = 300 s, T = 357°C; △, t_{O_2} = 900 s, T = 357°C) and on the form of surface oxygen t_{O_2} = 900 s, T = 388°C (○, first peak, i.e., chemisorbed oxygen; ●, second peak, i.e., PtO_2); reactor 3.

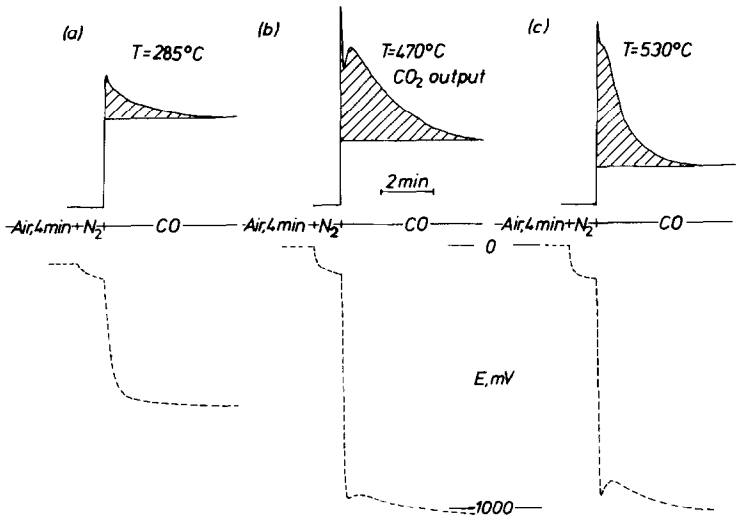

FIG. 13. Typical CO_2 and emf transients during surface titration experiments. Reactor 2. See text for discussion.

ences for $T = 388°C$ are 8×10^{-3} and 5.8×10^{-3} s^{-1}, respectively, in very good agreement with our measured value for PtO_2 desorption. The above authors report a very small, i.e., 1 kcal/mole, activation energy for PtO_2 reduction by CO. Despite this very good agreement it should be noted that the present results indicate that PtO_2 reduction by CO is faster than PtO_2 decomposition in a N_2 atmosphere. One can estimate the time constant of the reduction of PtO_2 by CO from the inverse of the time t^* elapsed between catalyst exposure to CO and appearance of the CO_2 maximum in the peak corresponding to PtO_2. No systematic study was performed on the effect of various parameters on t^*, but t^* values obtained in this study were of order 40 to 20 s at temperatures between 300 and 480°C (e.g., case b in Fig. 13 where $t^* = 26$ s). Consequently the rate constant for PtO_2 reduction by CO is of order 2.5×10^{-2} to 5×10^{-2} s in the above temperature range. This is a factor 4 to 8 higher than the values reported in Refs. (*22, 46*) and from those measured in the present work for PtO_2 decomposition in an inert atmosphere.

It is interesting to note the emf behavior upon catalyst exposure to CO when both chemisorbed oxygen and PtO_2 preexist on the catalyst surface. In this case, as shown in Fig. 13 (cases b and c), the emf exhibits an intermediate maximum during the transient which reflects a transient increase in the amount of chemisorbed oxygen. This chemisorbed oxygen must come from the dissociation of PtO_2. It is worth noting that such an intermediate transient emf maximum is not observed under conditions where PtO_2 does not preexist on the surface (Fig. 13 case a, where because of the low temperature, i.e., 285°C, practically no oxide has formed within the short O_2 exposure times, i.e., 4 min). The observation that PtO_2 decomposition is accompanied by an increase in emf, thus a transient increase in the amount of chemisorbed oxygen, is consistent with the similar emf behavior during the observed relaxation-type oscillations of the type A which appear on a preoxidized surface and apparently must correspond to PtO_2 decomposition. It should be noted that each of the three cases shown in Fig. 13 would correspond to a single point on Figs. 11 and 12.

As shown in Fig. 13 (case c) peak separa-

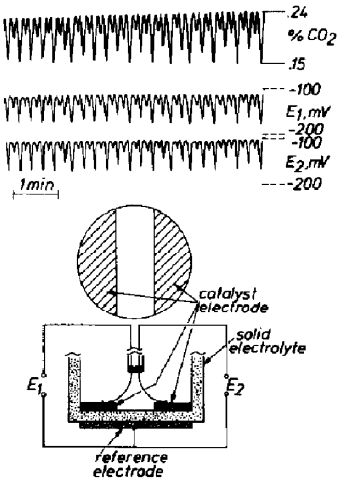

FIG. 14. Synchronization of rate and emf oscillations on two Pt catalyst films. Conditions: $p_{CO} = 4.9 \times 10^{-3}$ bar, $p_{O_2} = 4.2 \times 10^{-2}$ bar, $F = 3.45 \times 10^{-4}$ mole/s, $T =$ 283°C.

tion is not good at high temperatures. This must be due to the faster kinetics of PtO_2 decomposition and reaction with CO at high temperatures. In general peak separation was satisfactory between 300 and 450°C (e.g., Figs. 11 and 12). At low temperatures (e.g., Fig. 4 and case a in Fig. 13) the kinetics of PtO_2 formation are slow and very little PtO_2 formation takes place within short catalyst exposure times to oxygen t_{O_2} (1.7 and 4 min, respectively).

Communication and Synchronization of Crystallites during Oscillations

Figure 14 shows typical rate and emf results obtained during the course of the experiments with two Pt catalyst films present in the gradientless reactor. It can be seen that the surface oxygen activity on both films exhibits synchronous oscillations. The emf oscillations are also synchronous with the rate oscillations. The observed rate is, of course, the sum of the rates on both catalysts. The two catalyst–electrodes always behaved in an identical manner, both at steady state, at well-defined periodic relaxation-type oscillations and at apparently aperiodic oscillations of the type shown in Fig. 14. The two catalyst–electrodes were separated by a distance of roughly $l = 8$ mm and since stabilized zirconia is a good thermal insulator, the only means of communication of the two catalyst films is through the gas phase. Actually one can calculate that the characteristic time for heat conduction through the zirconia $t = l^2\rho C_p/K$, where ρ, C_p, and K are the density, specific heat, and thermal conductivity of stabilized zirconia, is of order 1 min which is an order of magnitude longer than typical experimentally observed rate relaxation time constants during oscillations. It therefore appears that fast mass transfer between adsorbed and gaseous species is the means of communication between different areas of a catalyst film during oscillations. There are two other conclusions which can be drawn from these experiments. One is that the reactor itself is indeed gradientless. The other is that changes in the gaseous composition during oscillations have a serious and immediate impact on surface concentrations and therefore inclusion of gas phase mass balances may be crucial in quantitatively describing oscillatory phenomena (*1, 5, 17*). Otherwise one cannot explain why the oscillations on the two films not only have the same waveform but also are synchronous; i.e., there is no detectable phase lag between the two signals.

Quantitative Steady-State Kinetics

The observed steady-state kinetic behavior is in qualitative agreement with many previous studies regarding the effect of p_{CO} and p_{O_2} on the reaction rate r (*1–5*). It was first attempted to describe the steady-state results, including the data which correspond to the baselines of type A and type B oscillations, by the classical Langmuir–Hinshelwood rate expression, assuming the surface reaction between chemisorbed CO and O to be rate controlling. It was found that no satisfactory fit to the data could be obtained either for the prereduced or for the preoxidized surface. This is not surpris-

ing in view of the fact that, as the emf data show, $a_O^2 < p_{O_2}$; thus adsorbed oxygen is not in equilibrium with gaseous oxygen. It was then found that both the steady-state kinetic results as well as the steady-state potentiometric results could be described very well by a steady-state model which is very similar to that of Sales *et al.* (*15*); i.e.,

$$O_2(g) + 2Pt \xrightarrow{k_{ad}} 2O - Pt \quad (9)$$

$$CO(g) + Pt \rightleftarrows CO - Pt \quad (10)$$

$$CO - Pt + O - Pt \xrightarrow{k_{LH}} CO_2 + 2Pt \quad (11)$$

where step (10) is in equilibrium. Assuming Langmuir-type adsorption on the oxide-free sites $1 - \theta_{ox}$ and neglecting the backward reaction terms of (9) and (11) one obtains

$$r = k_{ad} p_{O_2} \theta_u^2 (1 - \theta_{ox})^2 = k_{LH} \theta_{CO} \theta_O (1 - \theta_{ox})^2 \quad (12)$$

$$K_{CO} p_{CO} = \theta_{CO}/\theta_u, \quad (13)$$

where K_{CO} is the adsorption equilibrium constant of CO. After algebraic rearrangement and taking into account that $K_O a_O = \theta_O/\theta_u$ where K_O^2 is the dissociative adsorption equilibrium constant of O_2 and that

$$\theta_{CO} + \theta_O + \theta_u = 1 \quad (14)$$

one obtains

$$a_O = (k_{ad}/k_{LH} K_{CO} K_O) p_{O_2}/p_{CO} \quad (15)$$

$$r = (1 - \theta_{ox})^2 k_{LH}^2 k_{ad} K_{CO}^2 p_{CO}^2 p_{O_2}/(k_{ad} p_{O_2} + k_{LH} K_{CO} p_{CO} + k_{LH} K_{CO}^2 p_{CO}^2)^2. \quad (16)$$

Equation (15) is in good agreement with the experimentally observed dependence of a_O on gaseous composition, i.e., Eq. (7).

Equation (16) is also in good agreement with the kinetic results as shown in Figs. 5 and 7. To fit the kinetic data it was assumed that the coverage of PtO_2 is negligible on a prereduced surface, i.e., $\theta_{ox} = O$, and the resulting optimal values of the k_{ad}, k_{LH}, and K_{CO} were determined at each temperature separately. The experimentally determined temperature dependence of these parameters is shown in Table 1. The extracted activation energies are -1 kcal/mole for O_2 adsorption and 14 kcal/mole for the surface reaction. These values are in reasonable agreement with the literature (*8, 12, 22*). The temperature dependence of K_{CO} suggests values of 14 kcal/mole and -10 cal/mole · K for the heat and entropy of adsorption of CO, respectively. Both values are lower than those obtained from CO desorption experiments (*8*) but in good agreement with values extracted from kinetic CO oxidation data in the presence of chemisorbed oxygen (*39*).

TABLE 1

Temperature Dependence of k_{ad}, k_{LH}, K_{CO}, K'_{CO}, and θ_{ox} Values Used in the Kinetic Expression

	T(K)	θ_{ox}
$k_{ad} = 2.2 \times 10^{-4} \exp(1200/RT)$ mole/bar · s	557	0.30
$k_{LH} = 1.6 \exp(-14300/RT)$ mole/s	610	0.48
$K_{CO} = 7.4 \times 10^{-3} \exp(14100/RT)$ bar^{-1}	643	0.60
$K'_{CO} = 8.6 \times 10^{-4} \exp(15800/RT)$ bar^{-1}		
$n^0_{CO} = 3.6 \times 10^{-7}$ mole		
$R = 1.987$ cal/mole · K		

In order to fit the kinetic data on a preoxidized surface by Eq. (16) it is necessary to specify θ_{ox}. It was found that the kinetic data on a preoxidized surface could be described well by the same values of k_{ad} and k_{LH} extracted from the data on prereduced surfaces and with the θ_{ox} values shown in Table 1. However, it was found necessary to determine new values for the adsorption coefficient of CO and these values are denoted by K'_{CO} in Table 1. From the temperature dependence of K'_{CO} one estimates 16 kcal/mole and -14 cal/mole · K for the heat and the entropy, respectively, of CO chemisorption.

Once the parameters k_{ad}, k_{LH}, K_{CO}, and K'_{CO} have been kinetically determined, it is possible to examine the consistency of the proposed model by combining Eqs. (15) and (7) which describe the model predicted and experimentally determined dependence of a_O on temperature and gaseous composition. It follows from Eqs. (7) and (15) that

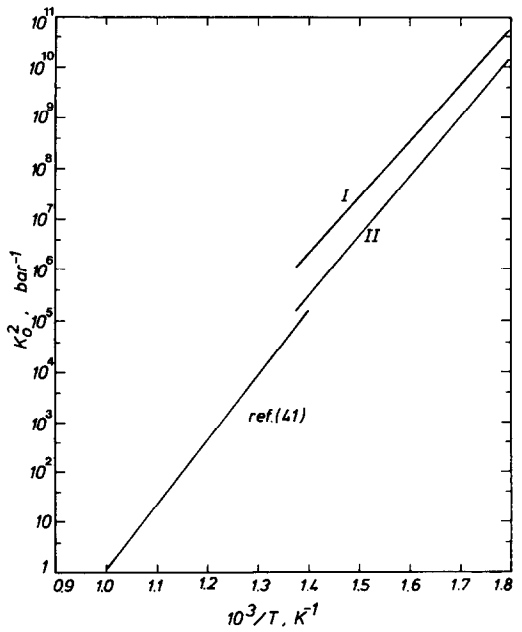

FIG. 15. Temperature dependence of K_O^2 on a preoxidized (I) and on a prereduced (II) surface and comparison with that obtained from i_O measurements (Ref. (*41*)).

on the fuel-lean side the adsorption coefficient K_O^2 for dissociative oxygen adsorption should equal $(k_{ad}/K_1 k_{LH} K_{CO})^2$ on a prereduced surface and $(k_{ad}/K_1 k_{LH} K'_{CO})^2$ on a preoxidized surface. Substituting from Table 1 one obtains $K_O^2 = 7.6 \times 10^{-12} \exp(54200/RT)$ and $K_O^2 = 5.6 \times 10^{-10} \exp(50900/RT)$ for a prereduced and a preoxidized surface, respectively. This suggest values of 50 to 55 kcal/mole and -40 to -50 cal/mole · K respectively for the heat and entropy of dissociative adsorption of oxygen. The $-\Delta H$ values are in good qualitative agreement with the literature (*1–5, 34, 40*) and the ΔS values also appear reasonable. The same comparison on the fuel-rich side gives similar reasonable values for ΔH but unreasonable (positive) values for ΔS. This indicates strongly that Eq. (5) does not hold exactly on the fuel-rich side.

The expressions extracted for the dissociative oxygen chemisorption coefficient on the fuel-lean side K_O^2 are in very good agreement with the direct measurements of Manton (*41*) as shown in Fig. 15. Manton used a three-electrode system of the type shown in Fig. 3b to measure the catalyst–electrode exchange current density i_O and its dependence on p_{O_2} and T, according to the elegant approach first used by Wang and Nowick (*43*). Since the i_O maxima with respect to p_{O_2} at constant T correspond to $\theta_O = \frac{1}{2}$ (*41, 43*) one can directly determine K_O^2 and measure its temperature dependence. The excellent agreement between K_O^2 measured by Manton (*41*) and that extracted from the present kinetic and potentiometric results strongly supports the basic validity of the proposed model.

It should be emphasized that the model presented here assumes the coverage of PtO_2 constant in time and therefore describes the steady-state kinetics only. In order to model the oscillations one must include the kinetics of formation and decomposition of PtO_2 and also include gas phase mass balances. Such a model will be presented in a forthcoming paper (*44*).

SUMMARY OF OBSERVATIONS AND DISCUSSION

The main new findings of the present investigation can be summarized as follows.

(I) Catalyst pretreatment has an important effect on both the steady-state and the oscillatory behavior of CO oxidation on Pt. At temperatures below 360°C the rate on a preoxidized surface is substantially lower than the rate on a prereduced surface. The steady-state kinetic behavior on a prereduced surface can be modeled quantitatively within the framework of Langmuir–Hinshelwood kinetics by considering that both the surface reaction between chemisorbed CO and atomic oxygen and the oxygen chemisorption step are rate limiting. Oxygen chemisorption is not in equilibrium during reaction as shown conclusively by the SEP measurements. The same kinetic model can successfully describe the kinetics on a preoxidized surface by assuming that a fraction of the catalyst surface is blocked by PtO_2. The model can also ex-

plain successfully the steady-state SEP measurements.

(II) Rate and emf oscillations are mostly of two types: Those produced on a preoxidized surface (type A) with rate and oxygen activity spikes "up" and those produced on a prereduced surface (type B) with rate and oxygen activity spikes "down." The baseline of type A and type B oscillations correspond to the steady-state rates on a preoxidized and on a prereduced surface, respectively. During oscillations these baselines are usually reached but never traversed by spikes originating from the other baseline. The same limits apply to AB-type oscillations and to aperiodic states. The frequency of type A oscillations increases with increasing p_{CO} and for low p_{O_2} also increases with p_{O_2}. On the contrary, the frequency of type B oscillations decreases with increasing p_{CO} but increases with increasing p_{O_2}. Increasing temperature has an increasing effect on the frequency both of type A and type B oscillations. Rate and emf oscillations were observed at temperatures between 240 and 400°C. The upper and lower temperature oscillation limits were found to increase with increasing p_{CO}/p_{O_2} in agreement with previous studies (*15, 22*).

During oscillations an increase in the rate is always accompanied by an increase in a_O, which is exactly the opposite of the behavior observed during ethylene oxidation rate and emf oscillations (*16, 17*). It is worth pointing out that oscillations of type A or type B or both have been observed in many previous studies. However, no distinction appears to have been made so far regarding their origin, i.e., preoxidized or prereduced catalyst surface.

(III) At the high-frequency bifurcation between oscillatory and nonoscillatory states the surface oxygen activity a_O is near the dissociation pressure of surface PtO_2, i.e., (*18, 45*),

$$\ln a_O = 12.5 - 12000/T. \qquad (17)$$

This is similar to the behavior observed during ethylene oxidation (*16, 17*) and underlines the important role played by surface PtO_2 in the mechanism of oscillatory phenomena during catalytic oxidations on Pt. That surface PtO_2 plays a central role in the oscillatory phenomena is further corroborated by a series of electrochemical oxygen pumping experiments published separately (*38*) which have shown that rate and emf oscillations of CO oxidation can be started or stopped at will by application of appropriate external voltages to the type of cell described here, i.e., by externally controlling the surface oxygen activity on the catalyst surface.

(IV) The existence of two types of oxygen bonded on the catalyst surface, i.e., dissociatively chemisorbed oxygen and PtO_2, has been demonstrated by a series of surface titration experiments at temperatures between 300 and 450°C. The two forms of oxygen appear as two distinct CO_2 peaks upon exposure of a preoxidized catalyst surface to CO. For long oxygen exposure times t_{O_2} the peak corresponding to PtO_2 was found to be up to a factor of 10 larger than the peak corresponding to chemisorbed oxygen, thus strongly indicating multilayer oxidation of the Pt catalyst surface. The above observations II, III, and IV together with the emf behavior during oscillations show conclusively that oscillations involve continuous oxidation and reduction of the Pt surface and support the basic validity of the Pt oxide model proposed to describe the atmospheric pressure rate oscillations of CO oxidation (*12, 15*). The present results, besides providing conclusive experimental support for the model, also suggest means for improving it, by including the PtO_2 decomposition pressure (Eq. (17)), by taking into account the possibility of multilayer Pt oxidation, and also by including gas phase mass balances. Such a model is presented in a forthcoming paper (*44*).

(V) The question frequently raised in the literature (*5*) about catalyst crystallite communication and synchronization has been

resolved by the two catalyst film experiments. These experiments have shown conclusively that catalyst crystallite communication and synchronization occur via fast mass transfer through the gas phase. This underlies the interplay between reactor and catalyst in the observed oscillatory phenomena, i.e., the correspondence between gas phase composition and surface composition oscillations. Without this means of crystallite communication via the gas phase no rate or emf oscillations would be macroscopically observable.

In summary the combination of detailed kinetic and SEP measurements together with isothermal surface titration experiments on Pt catalyst surfaces with carefully defined initial oxidation state appears to provide a self-consistent picture about the steady-state and oscillatory behavior of the atmospheric pressure CO oxidation on Pt and to support the validity of the PtO_2-based models for the description of the hysteresis and oscillatory phenomena of this system.

The present study shows the usefulness of solid electrolyte cells for the study of catalytic reactions on metals. The same type of cells can be used to control the oxidation state of the catalyst independently from the gas phase by appropriate application of external voltages. Results obtained with this active mode of operation for the oxidation of CO on Pt are presented in a separate paper (*38*).

ACKNOWLEDGMENTS

We thank the Stiftung Volkswagenwerk of the Federal Republic of Germany for financial support of this work through a Partnership Program Grant awarded to the Institut für Chemische Verfahrenstechnik of the University of Karlsruhe and to our Institute. We also thank Professors L. Riekert and H.-G. Lintz of the above Institute for numerous helpful discussions and their student Mr. H. Hildenbrand for grinding the thin solid electrolyte components. Sincere thanks are also expressed to Dr. J. J. Ehrhard for taking the XPS spectra.

REFERENCES

1. Sheintuch, M., and Schmitz, R. A., *Catal. Rev. Sci. Eng.* **15,** 107 (1977).
2. Slin'ko, M. M., and Slin'ko, M. G., *Catal. Rev. Sci. Eng.* **17,** 119 (1978).
3. Engel, T., and Ertl, G., *Adv. Catal.* **28,** 1 (1979).
4. Sheintuch, M., *J. Catal.* **96,** 326 (1985).
5. Razon, L. F., and Schmitz, R. A., *Catal. Rev. Sci. Eng.* **28,** 89 (1986).
6. Pikios, C. A., and Luss, D., *Chem. Eng. Sci.* **32,** 191 (1977).
7. Scheintuch, M., and Schmitz, R. A., *ACS Symp. Ser.* **165,** 487 (1978).
8. Dagonnier, R., and Nuyts, J., *J. Chem. Phys.* **65,** 2061 (1976).
9. Eigenberger, G., *Chem. Eng. Sci.* **33,** 1263 (1978).
10. Schmitz, R. A., *Proc. JACC* **2,** 21 (1978).
11. Boudart, M., Hanson, F. V., and Beegle, B., Paper presented at AIChE Meeting, Chicago, IL, November 1976.
12. Turner, J. E., Sales, B. C., and Maple, M. B., *Surf. Sci.* **103,** 54 (1981).
13. Turner, J. E., Sales, B. C., and Maple, M. B., *Surf. Sci.* **109,** 591 (1981).
14. Sales, B. C., Turner, J. E., and Maple, M. B., *Surf. Sci.* **112,** 272 (1981).
15. Sales, B. C., Turner, J. E., and Maple, M. B., *Surf. Sci.* **114,** 381 (1982).
16. Vayenas, C. G., Lee, B., and Michaels, J. N., *J. Catal.* **66,** 36 (1980).
17. Vayenas, C. G., Georgakis, C., Michaels, J. N., and Tormo, J., *J. Catal.* **67,** 348 (1981).
18. Vayenas, C. G., and Michaels, J. N., *Surf. Sci.* **120,** L405 (1982).
19. Ertl, G., Norton, R. P., and Rustig, J., *Phys. Rev. Lett.* **49,** 177 (1982).
20. Cox, M. P., Ertl, G., Imbihl, R., and Rustig, J., *Surf. Sci.* **134,** L517 (1983).
21. Imbihl, R., Cox, M. P., Ertl, G., Muller, H., and Brenig, W., *J. Chem. Phys.* **83,** 1578 (1985).
22. Yeates, R. C., Turner, J. E., Gellman, A. J., and Somorjai, G. A., *Surf. Sci.* **149,** 175 (1985).
23. Lindstrom, T. H., and Tsotsis, T. T., *Surf. Sci.* **167,** 1194 (1986).
24. Berry, R. J., *Surf. Sci.* **76,** 415 (1978).
25. Peuckert, M., and Ibach, M., *Surf. Sci.* **136,** 319 (1984).
26. Peuckert, M., and Bonzel, H. P., *Surf. Sci.* **145,** 239 (1984).
27. Hetrick, R. E., and Logothetis, E. M., *Appl. Phys. Lett.* **34,** 117 (1979).
28. Okamoto, H., Kawamura, G., and Kudo, T., *J. Catal.* **82,** 322 (1983).
29. Ehrhardt, J. J., Hafele, E., Lintz, H.-G., and Martins, A. F., *Ber. Bunsenges. Phys. Chem.* **89,** 894 (1985).
30. Hafele, E., and Lintz, H.-G., *Ber. Bunsenges. Phys. Chem.* **90,** 298 (1986).
31. Wagner, C., *Adv. Catal.* **21,** 323 (1970).
32. Stoukides, M., and Vayenas, C. G., *J. Catal.* **74,** 266 (1982).

33. Stoukides, M., and Vayenas, C. G., *J. Catal.* **82,** 45 (1983).
34. Barteau, M. A., Ko, E. I., and Madix, R. J., *Surf. Sci.* **102,** 99 (1981).
35. Riekert, L., *Ber. Bunsenges. Phys. Chem.* **85,** 297 (1981).
36. Vayenas, C. G., *J. Catal.* **90,** 371 (1984).
37. Razon, L. F., Chang, S. M., and Smith, R. A., *Chem. Eng. Sci.* **41,** 1561 (1986).
38. Yentekakis, I. V., and Vayenas, C. G., *J. Catal.*, **111,** 170–188.
39. Hori, G. K., and Schmidt, L. D., *J. Catal.* **38,** 335 (1975).
40. Campbell, C. T., Ertl, G., Kuipers, H., and Segner, J., *Surf. Sci.* **107,** 220 (1981).
41. Manton, M., Ph.D. thesis, Massachusetts Institute of Technology, 1986.
42. Yentekakis, I. V., Ph.D. thesis, University of Patras, 1987.
43. Wang, D. Y., and Nowick, A. S., *J. Electrochem. Soc.* **123**(1), 55 (1981).
44. Vayenas, C. G., and Ioannides, A., in preparation.
45. Vayenas, C. G., "Proc. 6th Intern. Conf. on Solid State Ionics, Garmisch-Partenkirchen, September 1987;" *Solid State Ionics,* in press.
46. Turner, J. E., and Maple, M. B., *Surf. Sci.* **147,** 647 (1984).